Recovery mechanisms of Arctic summer sea ice

S. Tietsche,[1] D. Notz,[1] J. H. Jungclaus,[1] and J. Marotzke[1]

Received 1 October 2010; revised 1 December 2010; accepted 14 December 2010; published 26 January 2011.

[1] We examine the recovery of Arctic sea ice from prescribed ice-free summer conditions in simulations of 21st century climate in an atmosphere–ocean general circulation model. We find that ice extent recovers typically within two years. The excess oceanic heat that had built up during the ice-free summer is rapidly returned to the atmosphere during the following autumn and winter, and then leaves the Arctic partly through increased longwave emission at the top of the atmosphere and partly through reduced atmospheric heat advection from lower latitudes. Oceanic heat transport does not contribute significantly to the loss of the excess heat. Our results suggest that anomalous loss of Arctic sea ice during a single summer is reversible, as the ice–albedo feedback is alleviated by large-scale recovery mechanisms. Hence, hysteretic threshold behavior (or a "tipping point") is unlikely to occur during the decline of Arctic summer sea-ice cover in the 21st century. **Citation:** Tietsche, S., D. Notz, J. H. Jungclaus, and J. Marotzke (2011), Recovery mechanisms of Arctic summer sea ice, *Geophys. Res. Lett.*, *38*, L02707, doi:10.1029/2010GL045698.

1. Introduction

[2] Arctic summer sea-ice extent has decreased substantially in recent years, and it will very likely continue to decrease owing to anthropogenic climate change. Because of the ice–albedo feedback, which reinforces the retreat, the transition from a perennial to a seasonal sea-ice cover might be associated with nonlinear threshold behavior. Nevertheless, other mechanisms stabilize Arctic summer sea-ice [*Notz*, 2009; *Eisenman and Wettlaufer*, 2009], and the present study investigates how these mechanisms lead to the recovery from prescribed ice losses in an atmosphere–ocean general circulation model (AOGCM) for the climate of the near future.

[3] The possibility of multiple equilibria and threshold behavior for polar ice caps, which implies the possibility of abrupt and irreversible changes in polar climate, has long been studied using energy balance models that incorporate the most relevant physical processes [*North*, 1984; *Merryfield et al.*, 2008; *Eisenman and Wettlaufer*, 2009]. The results of those studies, however, depend strongly on the choice and parameterization of large-scale processes. Therefore, studies with AOGCMs are desirable to decide if threshold behavior during the retreat of Arctic sea ice is a robust phenomenon. The IPCC-AR4 model runs provide a wealth of AOGCM projections of Arctic climate for the 21st century, and they do not exhibit clear evidence of a critical threshold for summer sea ice [*Winton*, 2006].

[4] Nevertheless, abrupt partial loss of Arctic summer sea ice is a common feature of those runs [*Holland et al.*, 2006]. Surprisingly, these abrupt partial losses are often followed by an equally rapid temporary recovery. This suggests that Arctic sea ice has a preferred equilibrium state that varies smoothly with the climatic forcing, and that there are recovery mechanisms that counteract the destabilizing ice–albedo effect after abrupt losses.

[5] A valuable tool for understanding those mechanisms are experiments which perturb Arctic sea-ice conditions systematically. To our knowledge, this sea-ice perturbation approach in an AOGCM has so far only been applied by *Schröder and Connolley* [2007], who showed that sea ice recovers from a complete removal within a few years. However, they restricted their experiments to a preindustrial climate and did not address the mechanisms of the sea-ice recovery.

[6] Here, we report the recovery of the Arctic from a prescribed loss of summer sea ice in the AOGCM ECHAM5/MPI-OM at different times during the 21st century, and investigate the mechanisms of recovery by analyzing the Arctic energy budget. In these perturbation experiments, the initial conditions are such that the ice–albedo feedback, as well as the other feedbacks related to sea-ice anomalies, are most pronounced. Thus, these experiments answer the question of whether perturbations of sea-ice cover alone are able to trigger an irreversible climate change in the Arctic.

2. Model and Experiments

[7] The global AOGCM we use consists of the atmosphere component ECHAM5 [*Roeckner et al.*, 2003] with a T31 horizontal resolution and 19 vertical levels, and the ocean component MPI-OM [*Marsland et al.*, 2003] with a curvilinear grid that has a horizontal resolution of 50–200 km in the Arctic and 40 vertical levels. A dynamic–thermodynamic sea-ice model based on the work by *Hibler* [1979] is included. The model setup we use is a coarse-resolution version of the IPCC-AR4 model described by *Jungclaus et al.* [2006]. This higher-resolution model setup has been tested extensively and performs well in simulating Arctic climate [*Chapman and Walsh*, 2007].

[8] We use ECHAM5/MPI-OM to perform a climate projection for the 21st century according to the IPCC-A1B emission scenario [*Nakićenović et al.*, 2000]. In this reference run, annual mean surface air temperature in the Arctic rises from −14°C in the 1900s to −4°C in the 2090s. Arctic sea-ice extent declines, and the Arctic Ocean is typically ice-free by the end of summer from 2070 onward (see auxiliary material[1]; we note that the sea-ice decline here is somewhat faster than in the higher-resolution version of the

[1]Max Planck Institute for Meteorology, Hamburg, Germany.

0094-8276/11/2010GL045698

[1]Auxiliary materials are available in the HTML. doi:10.1029/2010GL045698.

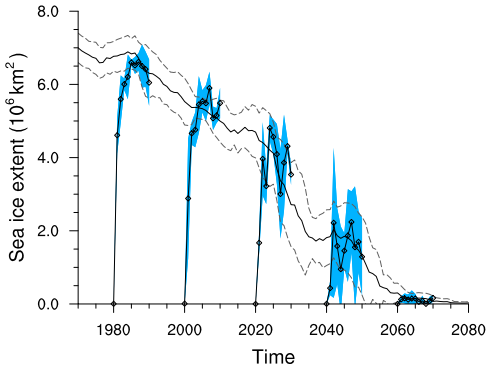

Figure 1. September Arctic sea extent. The thick black line is a 10-year moving average of the reference run, the dashed lines enclose the standard deviation of the reference run for the same 10-year window. The mean (diamonds) and the standard deviation (blue shading) of the perturbed model ensemble are shown at the year around which the ensemble is centered.

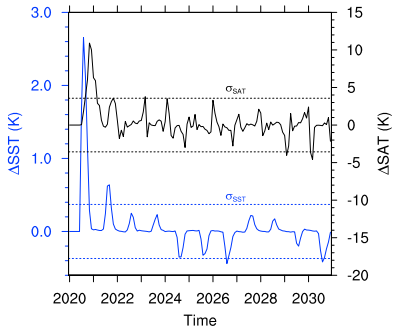

Figure 2. The 2020-ensemble mean of the difference in sea surface temperature (ΔSST) and surface air temperatures (ΔSAT) between the experiment and the reference run averaged over the Arctic Ocean domain. The dashed lines indicate the natural variability of the reference run, given by the standard deviation of September temperature in the 2020–2030 decade.

model). Between 2000 and 2040, when the rate of decline is maximal, Arctic summer sea-ice extent exhibits strong year-to-year fluctuations. As noted by *Holland et al.* [2008] and *Notz* [2009], this increase in variability is mostly due to changes in the ice thickness distribution and does not necessarily indicate proximity to some critical threshold.

[9] To examine the recovery mechanisms of Arctic summer sea ice, we simulate the consequences of an ice-free Arctic Ocean during summer. We set up experiments to start on 1st July from initial conditions that are taken from the reference run, but are perturbed by converting the entire Northern Hemisphere sea ice to water with the same properties as the sea surface water below the ice. Such conversion of relatively fresh sea ice to salty sea water has the advantage of leaving the properties of sea surface water unchanged. The start date is chosen such that the effect of the perturbation is maximal: starting from ice-free conditions earlier in the year leads to immediate re-freezing, and hence both earlier and later start dates imply shorter exposure of open water to sunlight, and a less pronounced ice–albedo effect.

[10] One might expect the Arctic Ocean to stay ice-free after the initial perturbation for several months, and possibly to stay seasonally ice-free in the following years because (i) in July air temperatures are usually above zero, and the ocean accumulates sensible heat throughout summer, (ii) the absence of sea ice implies a large excess of latent heat in the ocean surface layer, (iii) with sea ice absent, the ocean albedo is significantly lowered leading to increased shortwave absorption, and (iv) when cooling starts in autumn, the sea surface water will be more salty, causing convection to reach deeper and delay sea-ice formation.

[11] Every 20 years between 1980 and 2060, three such experiments are started in consecutive years (e.g., 2019, 2020, 2021), so that we can analyze five different time slices with a three-member ensemble each. After the initial perturbation, we let the model run freely without any further manipulation.

[12] In the following, we discuss the development of anomalies that arise due to the modified initial conditions, concentrating on field means over the Arctic Ocean and the atmospheric column above it. We define the Arctic Ocean domain to be bounded by the Bering Strait, the Fram Strait, and by the shortest connection from Spitsbergen to the northern end of Novaya Zemlya continued to the Siberian coast. The resulting area of the Arctic Ocean is $8.4 \cdot 10^{12}$ m^2.

[13] To characterize the time-dependent state of Arctic summer sea ice in the reference run, we quantify it by (i) the centered ten-year running mean of September sea-ice extent $\overline{X}(T)$ and (ii) the centered ten-year running standard deviation of September sea-ice extent $\sigma_X(T)$. We then consider sea-ice extent inside the range of $\overline{X}(T) \pm \sigma_X(T)$ to be typical for the reference run.

3. Results

3.1. Sea-Ice Extent and Temperature Anomalies

[14] All our experiments start from sea-ice free conditions on 1st July. As expected, the Arctic Ocean remains ice-free for several months, and significant sea-ice cover does not develop before November. However, sea ice then grows very rapidly, since the growth rate for thin ice is much higher than for thick ice, which acts as a negative feedback on thickness during the growth season [*Bitz and Roe*, 2004; *Notz*, 2009]. The ensemble mean September ice extent reaches values typical for the reference run in the fifth year after the perturbation for the 1980 time slice, in the fourth year for 2000, and already in the second year for 2020 and 2040 (Figure 1). September sea ice volume takes longer to recover in the late 20th century when the sea ice is still thick, but it has the same time scale of recovery as sea-ice extent from 2000 on (see auxiliary material). We conclude that there is no threshold in the changing reference state from which on the recovery of sea ice would be inhibited.

[15] Sea ice responds similarly to the initial perturbation in all time slices, and we consistently find the same mechanisms to be responsible for the recovery. Therefore, we keep the presentation concise and show only the analysis of the time-slice ensemble starting in 2019/20/21.

[16] We first consider anomalies in surface air temperature (SAT) and sea surface temperature (SST), because they are directly linked to the anomalies in sea-ice cover (Figure 2). At the sea surface, shortwave heating leads to a strong

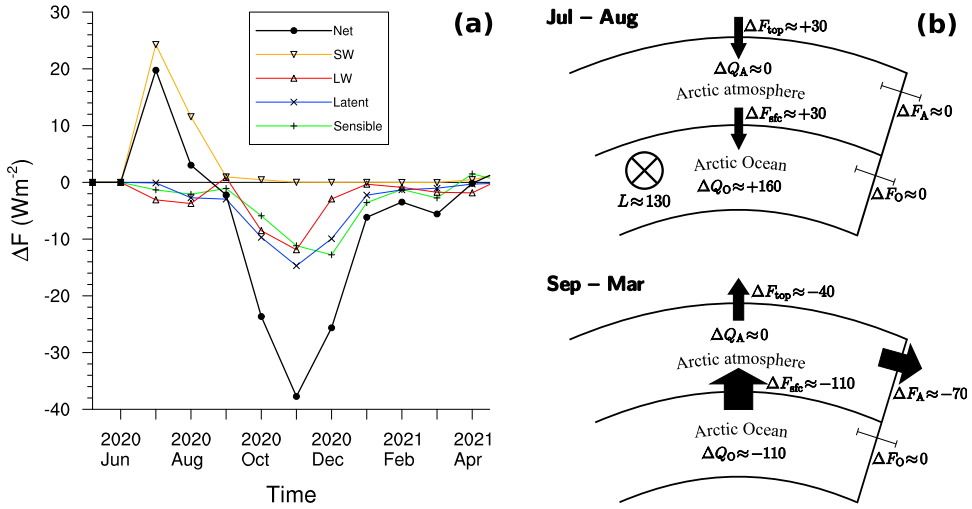

Figure 3. Mean energy budget anomalies for the Arctic Ocean domain. Shown are the values of the 2020 time slice experiments for the first nine months after starting from ice-free conditions on 1st July. (a) Downward surface heat flux anomaly. (b) Atmospheric and oceanic energy budget anomalies for the Arctic. All numbers are in energy units of 1 AEU ≡ $2.21 \cdot 10^{19}$J, which corresponds to the energy accumulated by a flux of 1 Wm^{-2} into the area of the Arctic Ocean domain during one month. Numbers are rounded to ten. Arrow widths are proportional to size of anomalies. (top) Summer phase from July to August. (bottom) Winter phase from September to March. Definition of symbols: ΔF_{top} is accumulated top-of-atmosphere net heat flux anomaly; ΔF_{sfc} is accumulated net surface heat flux anomaly; $\Delta F_{A/0}$ is accumulated atmospheric/oceanic lateral heat transport anomaly; $\Delta Q_{A/O}$ is the anomaly of atmospheric/oceanic heat content change; L is the latent heat anomaly of the ice-free initial conditions.

warming in the first summer of the experiment, and in the course of summer this temperature anomaly is mixed to an average depth of 50 m (see auxiliary material). However, the temperature anomaly does not penetrate deeper, and no excess heat is stored below the surface mixed layer. The water temperature in the uppermost ocean layer (12 m deep) shows a pronounced warming anomaly of 2.7 K, whereas the average temperature of the upper 50 m in the ocean rises by 1.3 K. We note that the magnitude of the ocean temperature anomaly is mainly due to the absence of melting ice that provides a latent heat sink. Without this effect, the surface heat flux anomaly would only warm the upper 50 m by 0.3 K.

[17] The SST anomaly only lasts until November; by then sufficient heat has been extracted from the surface water to cool it to the freezing temperature. Sea ice then forms from open water very rapidly, and partly recovers. In the next summer the sea-ice cover is still below normal, and larger shortwave absorption leads to a second positive SST anomaly. However, after the second year the SST anomalies are not larger than the natural variability of the reference run.

[18] For SAT a large positive anomaly occurs between October and February after the initial perturbation, with a peak of almost 11 K in November (Figure 2). After February, there are no further SAT anomalies stronger than natural variability. The warming is mainly restricted to the lower troposphere (see auxiliary material), which is a result that has also been found in GCM studies that prescribed permanent ice-free conditions in the Arctic Ocean [*Royer et al.*, 1990; *Winton*, 2008] and in observations of recent Arctic climate change [*Screen and Simmonds*, 2010]. The peak of the SAT anomaly occurs about four months later than the SST anomaly; the reason for this becomes clear when considering the energy budget.

3.2. Energy Budget of the Arctic Ocean Domain

[19] In the following, we examine accumulated heat fluxes and heat content changes for the Arctic Ocean domain. For ease of comparison, we introduce the Arctic energy unit 1 AEU ≡ $2.21 \cdot 10^{19}$J, which is the energy accumulated when a heat flux of 1 Wm^{-2} acts over the area of the Arctic Ocean domain ($8.4 \cdot 10^{12}$ m^2) for one average month (30.5 days). All numbers for energy budget anomalies are rounded to ten AEU, to account for uncertainty arising from energy budget residuals and ensemble spread. The Arctic energy budget anomalies in the experiments are summarized in Figure 3b, a schematic inspired by *Nakamura and Oort* [1988] and *Serreze et al.* [2007].

[20] We start our discussion of the energy budget anomalies with the oceanic heat transport. As shown by *Serreze et al.* [2007], heat transport into the Arctic Ocean by advection of warm water and export of sea ice is only between 4 and 7 Wm^{-2} (March and August mean, respectively). Our model shows comparable results for oceanic heat transport into the Arctic. When we compare the reference run to the perturbed run, no significant changes of oceanic heat transport are visible. This is plausible, since immediately after the perturbation, sea surface water has the same properties as in the reference run. During summer warming a temperature anomaly develops, and during winter freeze-up a salinity anomaly develops, but the resulting density anomaly is small compared to the seasonal cycle. Hence, we find that anomalies in oceanic heat transport into the Arctic are unimportant for the observed recovery of the Arctic energy budget.

[21] Consequently, the oceanic heat content anomaly is determined by the remaining two factors: (i) the latent heat anomaly induced by the initial conditions of the experiment and (ii) the surface heat flux anomaly. The latent

heat anomaly for the 2020 experiment has a magnitude of 130 AEU. The ability of the Arctic Ocean to store this excess heat over the course of winter is the key determinant for the evolution and stability of Arctic sea ice cover [*Serreze and Francis*, 2006]. When starting from ice-free conditions on 1st July, the ice–albedo effect at first reinforces the ocean heat content anomaly: net shortwave heat flux is strongly increased by about 25 Wm^{-2}, whereas the upward heat fluxes are only increased by 5 Wm^{-2} (Figure 3a). However, from September on the effect of shortwave flux is negligible, and the upward heat fluxes at the surface are increased with a peak anomaly of almost 40 Wm^{-2} in November. Thus, sea-ice free summer conditions cause the ocean to gain excess heat through the surface during summer, but they also cause enhanced heat loss through the surface in the following autumn and winter, when the insulating sea-ice cover is anomalously thin.

[22] The atmospheric energy budget anomaly is tightly coupled to the surface heat flux. During the summer phase from July to August, when the downward surface heat flux is amplified, the atmosphere only plays a passive role: the excess shortwave absorption of 30 AEU at the surface is balanced by an increase of net shortwave flux at the top of the atmosphere. Atmospheric heat content and lateral heat transport are not significantly affected (Figure 3b). However, during the longer winter phase from September to March, when the upward surface heat flux is amplified, the warming of the atmosphere leads to a decreased atmospheric heat transport into the Arctic Ocean domain by 70 AEU. At the same time, more longwave radiation is emitted at the top of the atmosphere, which accumulates to 40 AEU.

4. Conclusions

[23] In our perturbation experiments, we observe how different feedbacks in the Arctic compete to enhance or dampen a strong negative anomaly in sea ice, equivalent to a strong positive anomaly in oceanic heat content. In summer, the oceanic heat anomaly is enhanced by the ice–albedo feedback, but in winter the excess oceanic heat is lost to the atmosphere due to a lack of insulating sea-ice cover. This leads to an anomalously warm atmosphere, which in turn causes increased heat loss by longwave radiation at the top of the atmosphere and decreased heat gain by atmospheric advection from lower latitudes. A lasting impact of the ice–albedo feedback is not possible because the large-scale heat fluxes quickly adapt to release the excess oceanic heat from the Arctic.

[24] Hence, we find that even dramatic perturbations of summer sea-ice cover in the Arctic are reversible on very short time scales of typically two years. This suggests that a so-called tipping point, which would describe the sudden irreversible loss of Arctic summer sea ice during warming conditions, is unlikely to exist.

[25] These results also have implications for the value of sea-ice initial conditions for climate predictions on decadal time scales: if even the strong anomalies in sea-ice cover that we examine here are reversible within a few years, then small errors in sea-ice initial conditions should not affect the predictions significantly. Intrinsic memory of the thin Arctic sea-ice cover of the 21st century seems to span only a few years.

[26] **Acknowledgments.** We thank Wolfgang Müller for technical help and comments on the manuscript. This work was supported by the Max Planck Society and the International Max Planck Research School on Earth System Modelling. All simulations were performed at the German Climate Computing Center (DKRZ) in Hamburg, Germany.

References

Bitz, C. M., and G. H. Roe (2004), A mechanism for the high rate of sea ice thinning in the Arctic Ocean, *J. Clim.*, *17*, 3623–3632.

Chapman, W. L., and J. E. Walsh (2007), Simulations of Arctic temperature and pressure by global coupled models, *J. Clim.*, *20*(4), 609–632, doi:10.1175/JCLI4026.1.

Eisenman, I., and J. S. Wettlaufer (2009), Nonlinear threshold behavior during the loss of Arctic sea ice, *Proc. Nat. Acad. Sci. U. S. A.*, *106*(1), 28–32, doi:10.1073/pnas.0806887106.

Hibler, W. D., III (1979), A dynamic thermodynamic sea ice model, *J. Phys. Oceanogr.*, *9*(4), 815–846.

Holland, M. M., C. M. Bitz, and B. Tremblay (2006), Future abrupt reductions in the summer Arctic sea ice, *Geophys. Res. Lett.*, *33*, L23503, doi:10.1029/2006GL028024.

Holland, M. M., C. M. Bitz, L.-B. Tremblay, and D. A. Bailey (2008), The role of natural versus forced change in future rapid summer Arctic ice loss, in *Arctic Sea Ice Decline: Observations, Projections, Mechanisms, and Implications*, *Geophys. Monogr. Ser.*, vol. 180, edited by E. T. DeWeaver, C. M. Bitz, and L.-B. Tremblay, pp. 133–150, AGU, Washington D. C.

Jungclaus, J. H., N. Keenlyside, M. Botzet, H. Haak, J.-J. Luo, M. Latif, J. Marotzke, U. Mikolajewicz, and E. Roeckner (2006), Ocean circulation and tropical variability in the coupled model ECHAM5/MPI-OM, *J. Clim.*, *19*, 3952–3972.

Marsland, S. J., H. Haak, J. H. Jungclaus, M. Latif, and F. Röske (2003), The Max-Planck-Institute global ocean/sea ice model with orthogonal curvilinear coordinates, *Ocean Modell.*, *5*, 91–127.

Merryfield, W. J., M. M. Holland, and A. H. Monahan (2008), Multiple equilibria and abrupt transitions in Arctic summer sea ice extent, in *Arctic Sea Ice Decline: Observations, Projections, Mechanisms, and Implications*, *Geophys. Monogr. Ser.*, vol. 180, edited by E. T. DeWeaver, C. M. Bitz, and L.-B. Tremblay, pp. 151–174, AGU, Washington D. C.

Nakamura, N., and A. H. Oort (1988), Atmospheric heat budgets of the polar regions, *J. Geophys. Res.*, *93*(D8), 9510–9524.

Nakićenović, N., et al. (Eds.) (2000), *Special Report on Emissions Scenarios*, 559 pp., Cambridge Univ. Press, Cambridge, U. K.

North, G. R. (1984), The small ice cap instability in diffusive climate models, *J. Atmos. Sci.*, *41*(23), 3390–3395.

Notz, D. (2009), The future of ice sheets and sea ice: Between reversible retreat and unstoppable loss, *Proc. Nat. Acad. Sci. U. S. A.*, *106*(49), 20,590–20,595, doi:10.1073/pnas.0902356106.

Roeckner, E., et al. (2003), The atmospheric general circulation model ECHAM5, *Tech. Rep. 349*, Max Planck Inst. for Meteorol., Hamburg, Germany.

Royer, J. F., S. Planton, and M. Déqué (1990), A sensitivity experiment for the removal of Arctic sea ice with the French spectral general circulation model, *Clim. Dyn.*, *5*, 1–17.

Schröder, D., and W. M. Connolley (2007), Impact of instantaneous sea ice removal in a coupled general circulation model, *Geophys. Res. Lett.*, *34*, L14502, doi:10.1029/2007GL030253.

Screen, J. A., and I. Simmonds (2010), The central role of diminishing sea ice in recent Arctic temperature amplification, *Nature*, *464*(7293), 1334–1337.

Serreze, M. C., and J. A. Francis (2006), The Arctic amplification debate, *Clim. Change*, *76*, 241–264, doi:10.1007/s10584-005-9017-y.

Serreze, M. C., A. P. Barrett, A. G. Slater, M. Steele, J. Zhang, and K. E. Trenberth (2007), The large-scale energy budget of the Arctic, *J. Geophys. Res.*, *112*, D11122, doi:10.1029/2006JD008230.

Winton, M. (2006), Does the Arctic sea ice have a tipping point?, *Geophys. Res. Lett.*, *33*, L23504, doi:10.1029/2006GL028017.

Winton, M. (2008), Sea ice-albedo feedback and nonlinear Arctic climate change, in *Arctic Sea Ice Decline: Observations, Projections, Mechanisms, and Implications*, *Geophys. Monogr. Ser.*, vol. 180, edited by E. T. DeWeaver, C. M. Bitz, and L.-B. Tremblay, pp. 111–131, AGU, Washington D. C.

J. H. Jungclaus, J. Marotzke, D. Notz, and S. Tietsche, Max Planck Institute for Meteorology, Bundesstr. 53, D-20146 Hamburg, Germany. (steffen.tietsche@zmaw.de)